ARTICLES
https://doi.org/10.1038/s41557-020-00586-x
nature chemistry

Check for updates

# Protein folding modulates the chemical reactivity of a Gram-positive adhesin

Alvaro Alonso-Caballero[1,4] ✉, Daniel J. Echelman[1,2,4], Rafael Tapia-Rojo[1], Shubhasis Haldar[1,3], Edward C. Eckels[1] and Julio M. Fernandez[1]

**Gram-positive bacteria colonize mucosal tissues, withstanding large mechanical perturbations such as coughing, which generate shear forces that exceed the ability of non-covalent bonds to remain attached. To overcome these challenges, the pathogen *Streptococcus pyogenes* utilizes the protein Cpa, a pilus tip-end adhesin equipped with a Cys–Gln thioester bond. The reactivity of this bond towards host surface ligands enables covalent anchoring; however, colonization also requires cell migration and spreading over surfaces. The molecular mechanisms underlying these seemingly incompatible requirements remain unknown. Here we demonstrate a magnetic tweezers force spectroscopy assay that resolves the dynamics of the Cpa thioester bond under force. When folded at forces <6 pN, the Cpa thioester bond reacts reversibly with amine ligands, which are common in inflammation sites; however, mechanical unfolding and exposure to forces >6 pN block thioester reformation. We hypothesize that this folding-coupled reactivity switch (termed a smart covalent bond) could allow the adhesin to undergo binding and unbinding to surface ligands under low force and remain covalently attached under mechanical stress.**

In the ancient arms race between host and pathogen, bacteria have evolved novel adhesion strategies such as biofilm formation[1,2], non-covalent catch bond binding[3,4], and direct covalent binding to host substrates[5,6]. In particular, Gram-positive bacteria express a class of protein adhesins that contain internal Cys–Gln thioester bonds[5–7]. The thioester bond functions as an electrophilic substrate to draw a nucleophilic ligand, creating a covalent cross-link between a ligand and the adhesin of the bacterium[6]. Thioester bonds have evolved to permit bacterial adherence under large mechanical stresses[8]; however, bacterial colonization also benefits from cell rolling and spreading over surfaces[9,10], and the molecular mechanisms reconciling the interplay between mobility and covalent anchoring are not known.

We have recently demonstrated a novel assay to study the reactivity of the pilus-tip thioester adhesin Cpa from the Gram-positive pathogen *Streptococcus pyogenes* (*S. Pyogenes*)[11] (Fig. 1a), the causative agent of strep throat and necrotizing fasciitis[12]. Similar to our assays for disulfide bond mechanochemistry[13–15], our atomic force microscopy (AFM) force spectroscopy assay directly measured the presence or absence of the thioester bond in unfolding Cpa adhesins; however, due to technical limitations in AFM force spectroscopy[16], our assay could not probe how force regulated Cpa folding and its coupling with thioester mechanochemistry.

Here we demonstrate a novel magnetic tweezers force spectroscopy approach to resolve in detail the force dependency of the Cpa thioester bond reactivity in the 3–115 pN force range. Unlike AFM, magnetic tweezers possesses an incomparable stability that grants access to days-long recordings on the same molecule with millisecond and subpiconewton resolution[17,18]. Cpa is a mechanically stable protein[11] and, to apply high forces for long times, we design a novel double-covalent anchoring strategy based on HaloTag chemistry and the SpyCatcher/SpyTag split-protein technique[19–21], which allows for the end-to-end covalent immobilization of single Cpa polyprotein molecules. This technical advance enables us to explore different conditions on the same molecule without probe detachment, a limiting factor in force spectroscopy experiments[22–25]. With these improvements, we now determine the force dependency of Cpa folding and its relation to thioester bond cleavage by the nucleophile methylamine. We find that methylamine-induced cleavage is inhibited at forces >35 pN, whereas thioester reformation and ligand uncoupling occur at forces <6 pN. Our observations indicate that protein folding is a prerequisite for thioester reformation, which suggests an allosteric role of folding on the reactivity of this bond. We hypothesize that the force ranges over which thioester reformation and Cpa folding occur could indicate a novel mechanism to respond to varying levels of shear stress. Under high-force conditions, the adhesin–ligand covalent interaction can withstand forces over 1,000 pN. When the mechanical stress eases up, the folding of the Cpa parent protein, at 6 pN or less, reestablishes the thioester bond reactivity by enabling its cyclic reformation and ligand-induced cleavage by surface ligands. We dub such folding-controlled covalent reactivity as smart covalent bonds. In the current context of antibiotic resistance[26], targeting the bacterial adhesion molecules stands out as a promising strategy to battle infections[27], especially considering the difficulties treating infections caused by Gram-positive pathogens[28]. In such an effort, we identify a mechanism for the abrogation of Cpa thioester bond reactivity towards surface ligands, based on the oxidation of the side-chain thiol of the Cys residue involved in the thioester bond. A better understanding of the adhesive chemistries of Gram-positive pathogens will permit the rational development of novel classes of antibiotics and vaccines, which is of great importance to society.

## Results

**Double-covalent magnetic tweezers anchoring.** We use a polyprotein of the domains $CnaB_{D595A}$(M)–TED(T) of this adhesin to explore Cpa thioester bond mechanochemistry (Fig. 1a,b), as we previously described[11]. The Cys426–Gln575 thioester bond

[1]Department of Biological Sciences, Columbia University, New York, NY, USA. [2]Present address: Boston Combined Residency Program, Boston Children's Hospital, Boston, MA, USA. [3]Present address: Ashoka University, Haryana, India. [4]These authors contributed equally: Alvaro Alonso-Caballero, Daniel J. Echelman. ✉e-mail: aa3995@columbia.edu

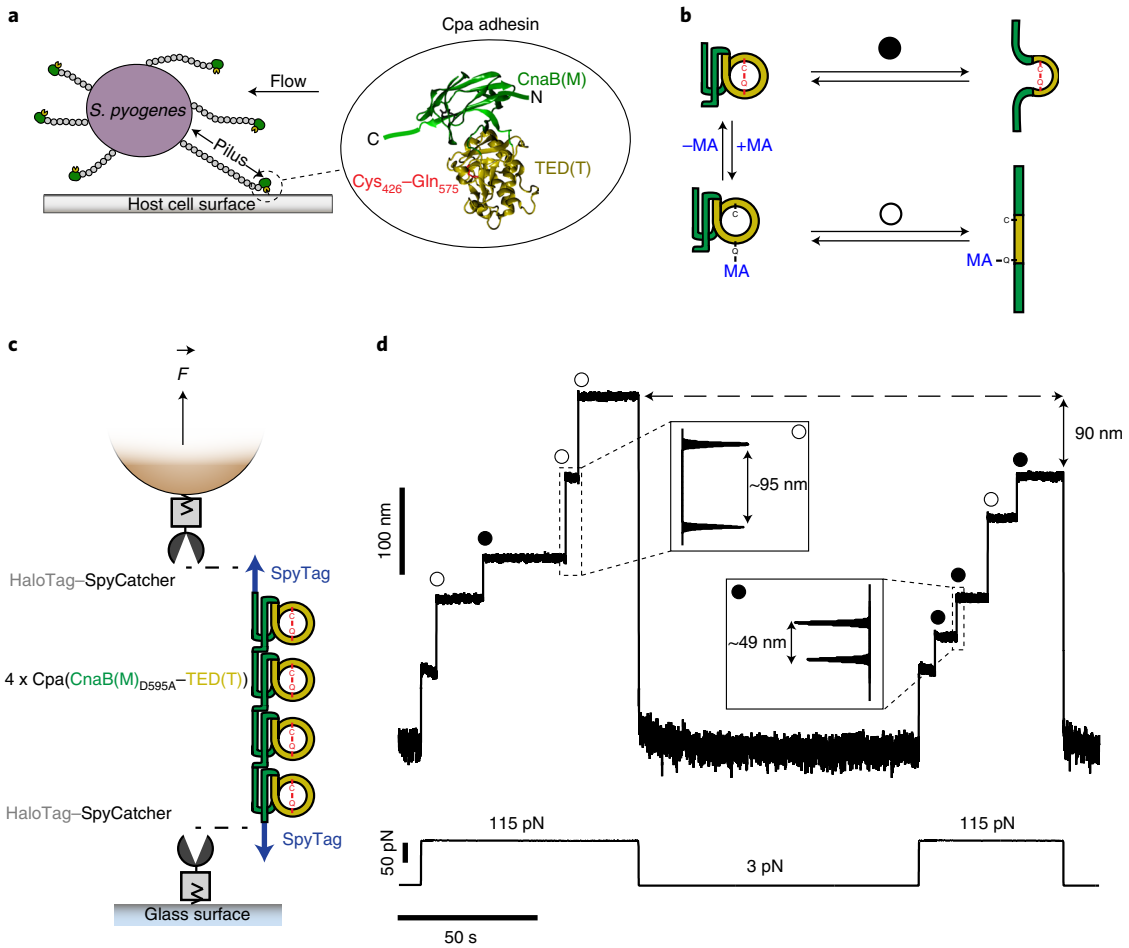


**Fig. 1 | Mechanochemistry of *S. pyogenes* Cpa adhesin. a**, *S. pyogenes* attach to host cell surfaces via the Cpa protein, which is present in the tip-end of the pili. The Cpa main core comprises the CnaB(M) domain (green), in whose fold the TED(T) domain is inserted (yellow). The TED(T) domain contains a thioester bond formed between the residues Cys426 and Gln575 (red), which mediates the attachment to cell-surface molecules. **b**, In the folded state, nucleophiles such as methylamine (MA) can cleave the thioester bond and bind covalently to the Gln side-chain (+MA); however, thioester bond reformation and ligand uncoupling (−MA) can occur. After mechanical extension, the presence (black circle pathway) or absence (empty circle pathway) of the thioester bond can be assessed as a difference in the extension of the protein. **c**, The double-covalent magnetic tweezers experimental assay is shown. Protein anchors HaloTag–SpyCatcher are covalently immobilized both to the surface of the glass and the paramagnetic bead. A chimeric polyprotein made of four copies of Cpa and flanked by SpyTag peptides is covalently linked to the glass and the bead through the reaction of the SpyCatcher/SpyTag split protein system. On the top of the scheme (not shown), the position of a pair of magnets is controlled for the application of calibrated forces to the tethered molecule. *F*, force. **d**, A magnetic tweezers recording of a Cpa polyprotein exposed to 100 mM methylamine, where the extension of the molecule is registered across time. A force pulse of 115 pN leads to the mechanical unfolding of the four Cpa domains, which is detected as stepwise increases in the extension. Here, three of the domains lack their internal thioester bond (empty circles) yielding an extension of ~95 nm, whereas one of the domains preserves its thioester bond (black circle) and yields an unfolding extension of ~49 nm. Following a 100-s-long quench force pulse at 3 pN, which favours both folding and bond reformation, a second 115 pN pulse reveals that two Cpa domains reformed their thioester bonds (black circles), decreasing the final extension of the polyprotein by 90 nm, as a consequence of the polypeptide sequence trapped by the newly formed bonds.

resides within the TED domain (thioester domain), whose fold is contained inside of the fold of the CnaB domain (Fig. 1a). The D595A mutation prevents the formation of the native isopeptide bond present in the CnaB(M) domain and thus the CnaB(M) domain can be mechanically unfolded when pulled from its N and C termini, which allows us to apply force to the TED(T) domain and evaluate the presence, absence or real-time ligand-induced rupture of the thioester bond. Despite the absence of the native isopeptide bond, this protein still exhibits high mechanical stability and requires the application of high forces for unfolding. To solve this problem, we develop a strategy to covalently anchor Cpa polyproteins both to the glass surface and the magnetic probes of a magnetic tweezers set-up. Both glass and probe surfaces are independently functionalized with the HaloTag ligand, which permits the covalent immobilization of HaloTag proteins[17,19,20]. First we immobilize the chimeric protein SpyCatcher–HaloTag onto the glass and on the bead surface. We then add the chimeric polyprotein SpyTag–$(CnaB_{D595A}–TED)_4$–SpyTag to the glass surface, allowing the reaction with the SpyCatcher–HaloTag present on the surface. The SpyCatcher/SpyTag split-protein system reacts to form an intermolecular isopeptide bond between the SpyTag and the SpyCatcher counterpart[21,29,30], covalently connecting both chimeric proteins. Finally, we close this assembly by adding functionalized paramagnetic beads, whose surface-bound SpyCatcher–HaloTag protein reacts with the SpyTag peptide present on the free end of the Cpa polyprotein (Fig. 1c). After capping, the Cpa polyprotein becomes covalently tethered both to the glass and bead surfaces.

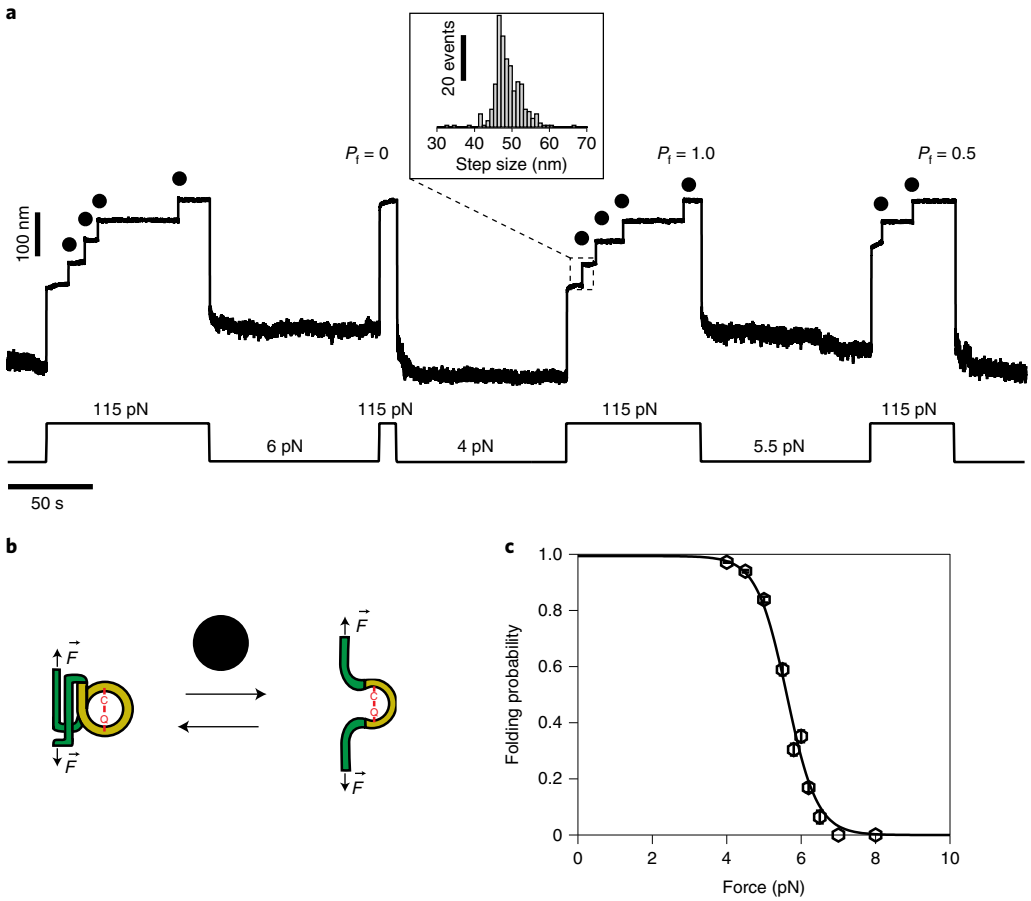


**Fig. 2 | Dynamics of the thioester-intact Cpa polyprotein under force. a**, The magnetic tweezers trajectory of the Cpa polyprotein. High force pulses at 115 pN unfold the thioester-intact Cpa domains, which show 48.8 ± 3.8 nm (mean ± s.d., $n = 272$) stepwise extensions (inset histogram). Low force pulses of 100-s-long allow Cpa refolding, enabling us to determine the folding probability ($P_f$) at different forces. As an example, a quench at 6 pN does not allow folding of any of the domains, whereas four fold at 4 pN ($P_f = 1.0$) and only two fold at 5.5 pN ($P_f = 0.5$). **b**, A cartoon representation of the folding–unfolding of the Cpa domain. The thioester bond between Cys426 and Gln575 clamps the TED domain (yellow), limiting its extensibility. **c**, The folding probability of thioester-intact Cpa. Data points are fitted to a sigmoidal function and they represent the probability at each of the forces tested for 100 s ($n = 54$ at 4 pN; $n = 30$ at 4.5 pN; $n = 18$ at 5 pN; $n = 16$ at 5.5 pN; $n = 16$ at 5.8 pN; $n = 23$ at 6 pN; $n = 14$ at 6.2 pN; $n = 10$ at 6.5 pN; $n = 9$ at 7 pN; $n = 5$ at 8 pN). Data points are the mean and the bars are the s.d., calculated using jackknife analysis.

The magnetic tweezers experiment starts when the protein-bound paramagnetic bead is exposed to a magnetic field[17]. The presence or absence of the thioester bonds in the Cpa polyprotein can be easily detected as a difference in the unfolding extensions (Fig. 1b). Figure 1d shows a magnetic tweezers trajectory of a Cpa polyprotein that has been previously exposed to a solution containing 100 mM methylamine (Hepes 50 mM pH 8.5, NaCl 150 mM, ascorbic acid 10 mM, EDTA 1 mM). The application of a constant force of 115 pN leads to the sequential unfolding of the Cpa polyprotein, yielding stepwise increases in length of different sizes: one corresponding to thioester-bond-intact proteins (~49 nm), and three corresponding to thioester-bond-cleaved proteins (~95 nm). The force was subsequently reduced to 3 pN to allow the folding of Cpa and also the reformation of the thioester bonds. A second 115 pN pulse reveals that two more Cpa domains reformed their bonds (~49 nm steps) and the total extension of the polyprotein thus decreases by 90 nm, as the formation of these two thioester bonds prevents the full extension of the protein. The different extensions of Cpa—depending on the presence or absence of its internal thioester bond—serve to clearly identify the status of the bond.

**Force-dependency of the thioester bond cleavage and reformation.** The mechanical unfolding of the $CnaB_{D595A}$–TED domains with the thioester bond intact remains limited to the polypeptide sequence not trapped by the bond. This accounts for a total of 164 residues located before the Cys426 and after the Gln575, which corresponds to the ~49 nm steps observed in Fig. 1d. In a nucleophile-free solution, the polyprotein unfolding at 115 pN reveals stepwise increases in length of 48.8 ± 3.8 nm (mean ± s.d.), as it can be seen in the trajectory of Fig. 2a. In these unfolding extensions, the entire CnaB fold and a small region of the TED domain (the TED fold spans from residues Ala393 to Gly579, and the sequence sequestered by the thioester bond spans from Cys426 to Gln575) unfold as a unique step; however, pulling at lower forces allows to separate the unfolding of these two regions, revealing a short-lived intermediate state as we previously reported[11] (Supplementary Fig. 1). Due to the exquisite force resolution of magnetic tweezers, we can explore not only the Cpa polyprotein unfolding at high forces, but also the reversible process of folding at low forces (Fig. 2b). As can be seen in Fig. 2a, a quench for 100 s at 6 pN and a subsequent pulling pulse at 115 pN shows no evidence of protein folding ($P_f = 0$). On the contrary, holding the protein at 4 pN for the same amount of time is enough to completely fold the thioester-intact Cpa polyprotein ($P_f = 1.0$), whereas only half of the domains could fold at 5.5 pN ($P_f = 0.5$). In this manner we determine the folding probability of the thioester-intact polyprotein, which shows a sharp transition

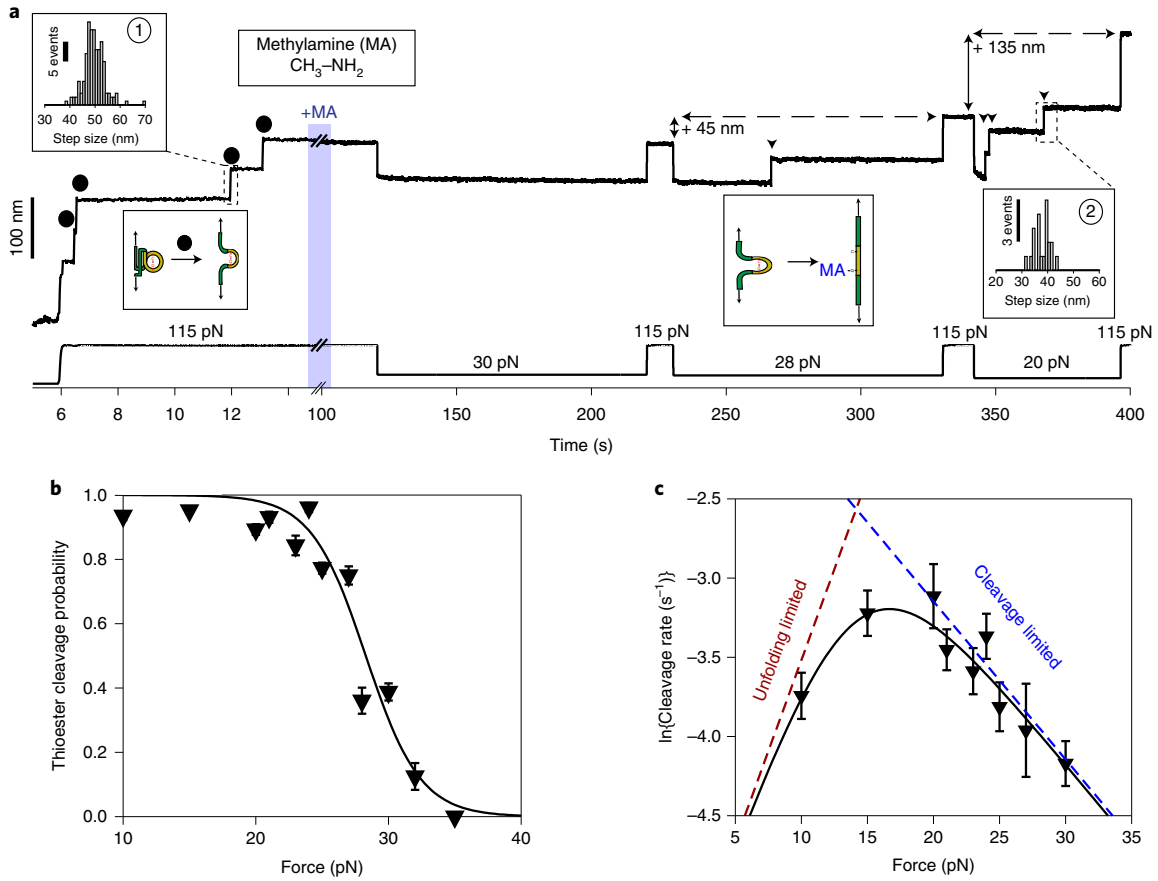


**Fig. 3 | Cpa thioester bond cleavage is negatively force-dependent. a**, The magnetic tweezers trajectory of the Cpa polyprotein. After the unfolding of the thioester-intact Cpa domains at 115 pN (black circles; histogram inset 1: 49.6 ± 4.1 nm, mean ± s.d., $n$ = 164), the buffer is exchanged to a Hepes solution containing 100 mM methylamine (+MA). At high force, no additional steps are registered as would be expected from a thioester bond cleavage event. We thereafter apply a protocol with subsequent pulses of decreasing mechanical load to investigate the force dependency of the reaction. Although no cleavage is observed at 30 pN, 100 s at 28 pN reveals one step that comes from the methylamine-induced cleavage of the thioester bond of one of the four Cpa domains (triangle). At 115 pN, the final extension of the molecule has increased by 45 nm, which originates from the polypeptide sequence released after thioester bond lysis. When held at 20 pN, the three remaining thioester bonds are cleaved (triangles; histogram inset 2: 38 ± 3.1 nm, mean ± s.d., $n$ = 21) and the final extension of the molecule increases for another 135 nm. **b**, Thioester bond cleavage probability as a function of force measured over a 100 s time-window. Data points are the mean and the error bars are the s.d. calculated using jackknife analysis. The line represents a sigmoidal fit to the data ($n$ = 12 at 10 pN; $n$ = 20 at 15 pN; $n$ = 15 at 20 pN; $n$ = 9 at 21 pN; $n$ = 10 at 23 pN; $n$ = 9 at 24 pN; $n$ = 15 at 25 pN; $n$ = 15 at 27 pN; $n$ = 7 at 28 pN; $n$ = 15 at 30 pN; $n$ = 5 at 32 pN; $n$ = 6 at 35 pN). **c**, The rate of thioester bond cleavage as a function of force. Data points show the natural logarithm of the cleavage rate and the bars show the standard error of the mean. The curve represents a fit to the data described by a model that takes into account the effect of two sequential reactions: the rate of protein unfolding, which increases with force, and the rate of thioester bond cleavage, which decreases with force. From this fit, we obtain a distance to the transition state for TED protein unfolding ($x_U^{\ddagger}$) of 0.9 nm, whereas the thioester bond cleavage exhibits a negative distance to the transition state ($x_C^{\ddagger} = -0.4$ nm), which suggests a requirement of a contraction of the Cpa polypeptide substrate to proceed with the cleavage of the bond, explaining its negative force dependence. The dotted lines represent the individual unfolding and cleavage rates as obtained from the fit to the proposed model (Supplementary Equation (3), see Methods) ($n$ = 30 at 10 pN; $n$ = 38 at 15 pN; $n$ = 24 at 20 pN; $n$ = 23 at 21 pN; $n$ = 23 at 23 pN; $n$ = 24 at 24 pN; $n$ = 21 at 25 pN; $n$ = 37 at 27 pN; $n$ = 15 at 30 pN). Rate versus force-dependency data was obtained in unrestricted time-window experiments.

from fully folded at 4.5 pN to completely unfolded at 6.5 pN (Fig. 2c). Cpa mechanical unfolding in the absence of nucleophiles therefore yields a homogeneous population of steps of ~49 nm, which confirms that over the explored range of forces the thioester bond remains inert.

The stability of magnetic tweezers and the double-covalent anchoring of the protein allow us to exchange the solution in the experimental fluid chamber, enabling us to explore the reactivity of the thioester bond under force while under different conditions; hence, we change to a solution containing 100 mM methylamine, which we add after the mechanical unfolding of the thioester-intact Cpa, as shown in Fig. 3a. At 115 pN, the addition of methylamine does not yield any additional extension increase, indicating the lack of reactivity of the thioester bond at high forces. Taking advantage of the magnetic tweezers force resolution, we apply a protocol with consecutive decreasing force pulses of 100 s to elucidate the force-range reactivity of this bond in real time. Initially, decreasing the force to 30 pN does not alter the thioester bond state, as can be seen from the following 115 pN pulse where the same final extension of the molecule is reached. By contrast, applying a pulse of 28 pN reveals one discrete step originating from the bond cleavage of one of the four Cpa proteins. When we stretch again at 115 pN, the final extension of the molecule increases by 45 nm, which confirms this observation. This additional length comes from the release of the polypeptide sequence sequestered by the Cys426–Gln575, which scales with the number of residues previously

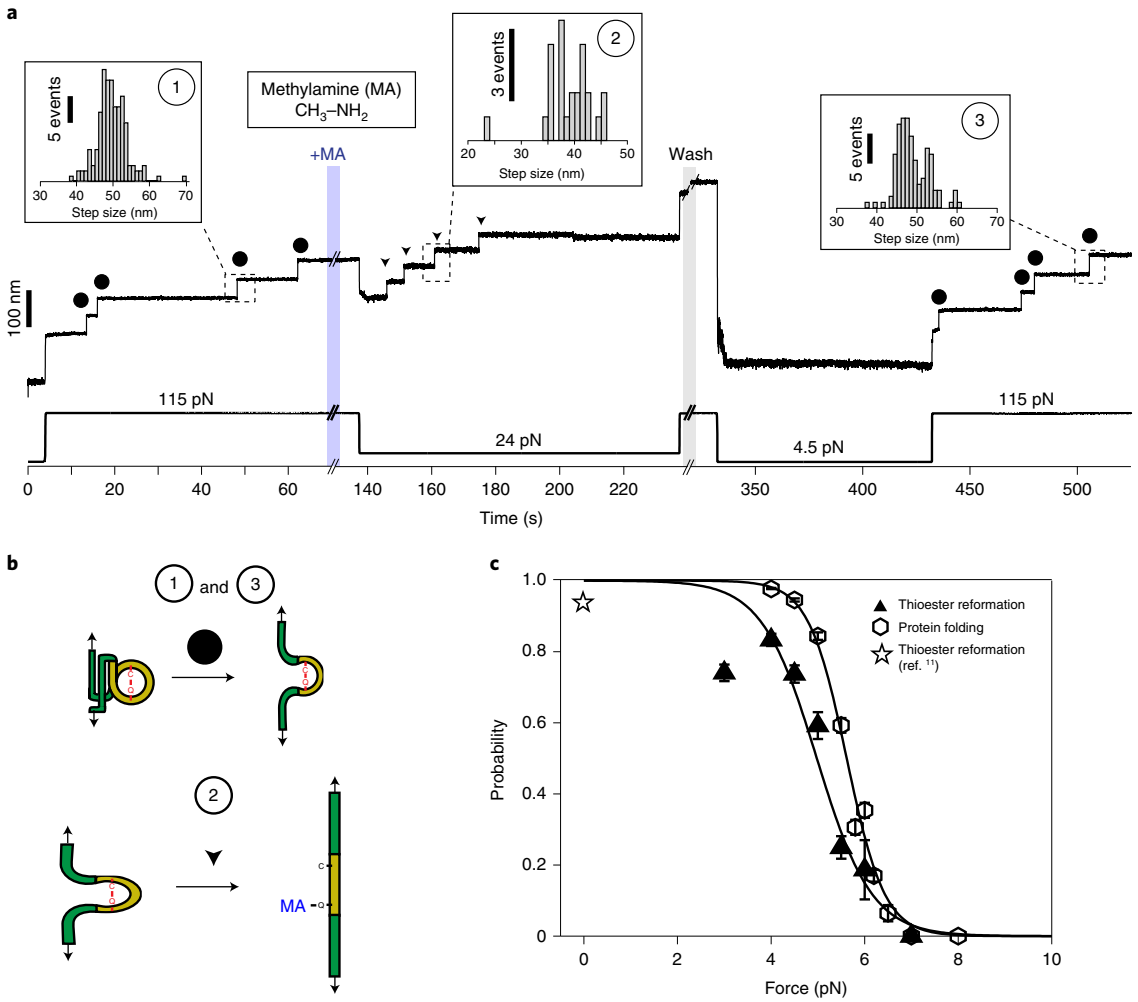


**Fig. 4 | Protein folding drives thioester bond reformation. a**, Magnetic tweezers trajectory of the Cpa polyprotein. After the unfolding of the thioester-intact Cpa domains at 115 pN (circles; inset histogram 1: 49.6 ± 4.1 nm, mean ± s.d., $n = 164$), the buffer is exchanged and the polyprotein is exposed to a solution containing 100 mM methylamine (+MA). As expected, we do not observe cleavage at this high force, but a drop to 24 pN permits the full cleavage of the four candidate thioester bonds (triangles, inset histogram 2; 38.8 ± 4.4 nm for 24 pN, mean ± s.d., $n = 25$). To study the reformation of the bond, we remove the nucleophile-containing buffer at high force and quench the force to 4.5 pN for 100 s to favour bond reformation and protein folding. We stretch again the polyprotein at 115 pN and identify four thioester-intact Cpa domains, which indicates that the four cleaved candidates were able to fold and reform their bonds (circles; inset histogram 3: 48.8 ± 4.1 nm, mean ± s.d., $n = 117$). **b**, A cartoon representation of the extension events registered on the Cpa trajectory shown in **a**. Events 1 and 3 show the mechanical extension at 115 pN of thioester-intact Cpa, before cleavage and after reformation, respectively. Event 2 shows the extension after methylamine (MA) cleavage at 24 pN. **c**, Comparison between the thioester bond reformation (upwards triangles and sigmoidal fit) and the thioester-intact Cpa folding probability (hexagons and sigmoidal fit, from Fig. 2c) as a function of the mechanical load. The star sindicates the reformation probability obtained at 0 pN from our previous work with AFM[11]. Data points for reformation are the mean and the error bars are the s.d. calculated using jackknife analysis. Reformation registered as the amount of thioester-intact domains after methylamine washout and after a 100 s time-window at the folding/reformation force range ($n = 13$ at 3 pN; $n = 16$ at 4 pN; $n = 15$ at 4.5 pN; $n = 12$ at 5 pN; $n = 6$ at 5.5 pN; $n = 7$ at 6 pN; $n = 6$ at 7 pN).

trapped by the bond and also with the applied force following the freely jointed chain model for polymer elasticity[31] (Supplementary Fig. 2). Finally, dropping the force to 20 pN leads to the rapid cleavage of the three remaining bonds in the polyprotein, yielding three steps of 38 ± 3.1 nm (mean ± s.d., inset histogram 2). Exploring the range from 10 to 35 pN, we determine that thioester bond cleavage does not occur over a 100 s time-window if Cpa is exposed to forces >35 pN. When held at lower forces, stepwise increases in length occur due to thioester bond cleavage, reaching completion in 100 s at forces <23 pN (Fig. 3b), which indicates a negative force dependency in the ligand-induced cleavage. We sought to delve into the kinetics of thioester bond cleavage by measuring the rates of bond cleavage as a function of force (with no time-window limits) in the range spanning from 10 to 30 pN, as we show in Fig. 3c. We observe that the rate of cleavage is optimum at ~20 pN, above which it decreases, as expected from our observations in 100 s time windows (Fig. 3b). At lower forces this tendency is reversed. This behaviour can be explained in the context of two sequential processes with opposite force dependencies: the chemical cleavage of the bond and the mechanical unfolding of the protein. In these experiments, our observational event is the unfolding of the TED domain after the cleavage of its thioester bond by methylamine. To observe the extension of the TED domain, the chemical cleavage of the thioester bond has to occur before. Assuming the Bell model for bond lifetimes under force[32], we elaborate a model (see the Methods for a detailed description) that accounts for the rates of protein unfolding

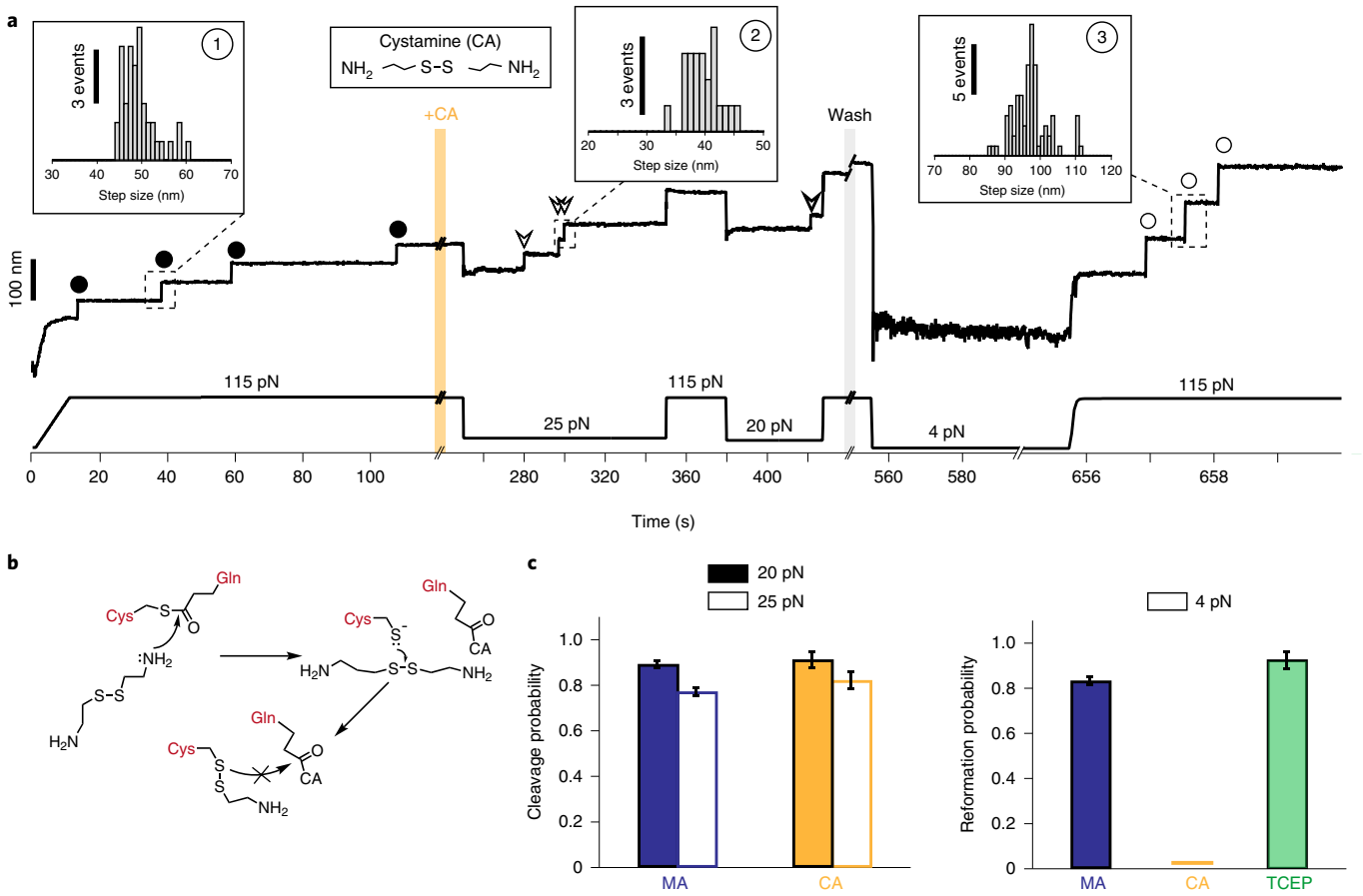


**Fig. 5 | Cystamine-mediated abrogation of Cpa thioester bond reformation. a**, The magnetic tweezers trajectory of the Cpa polyprotein. After the unfolding of the thioester-intact Cpa domains at 115 pN (circles, inset histogram 1; 49.3 ± 3.8 nm, mean ± s.d., $n = 42$), the buffer is exchanged and the polyprotein is exposed to a solution containing 100 mM cystamine (+CA). At 115 pN, no additional extensions are registered, but a drop in the force to 25 pN for 100 s leads to the appearance of three steps that account for the release of the polypeptide sequence trapped by the thioester bonds (empty arrows, inset histogram 2; 39.6 ± 2.7 nm for 25 pN, mean ± s.d., $n = 23$). After cleavage of all the bonds and after CA washout, force is quenched to 4 pN for 100 s to favour folding and reformation of the thioester. The final 115 pN pulse reveals three steps corresponding to thioester bond-cleaved Cpa domains (empty circles, inset histogram 3; 97.1 ± 5.2 nm, mean ± s.d., $n = 78$). **b**, A chemical scheme depicting the reformation blocking effect of CA. After the thioester bond nucleophilic cleavage by one of the CA primary amines, the free Cys thiol can attack the CA disulfide bond (from the bound CA, or from another CA molecule). As a result, an intermolecular disulfide bond between Cpa Cys426 and CA is formed, preventing the thioester bond reformation. This disulfide reshuffling breaks the CA molecule and generates one free CA molecule (not shown in the scheme) and a Cys426-bound CA. **c**, The left plot compares the thioester bond cleavage probability by methylamine (MA) and CA at 20 and 25 pN (MA, $n = 15$ at 20 pN, $n = 15$ at 25 pN; CA, $n = 8$ at 20 pN, $n = 9$ at 25 pN), whereas the right plot compares the thioester bond reformation probability after 100 s at 4 pN after the treatment with MA, CA and CA followed by TCEP (MA, $n = 16$; CA, $n = 17$; TCEP, $n = 6$). Histogram bars are the mean and the error bars are the s.d. calculated using jackknife analysis.

and the chemical cleavage of the bond. Chemical cleavage is favoured at forces <20 pN; however, the mechanical unfolding of the TED domain is limiting. By contrast, at forces above 20 pN, the mechanical unfolding of the TED domain is increasingly favoured but the chemical cleavage process is hindered and therefore slowed down. This model correctly describes the behaviour observed, and predicts a positive distance to the transition state of ~0.9 nm for the unfolding of the TED domain, and a negative distance to the transition state for the chemical cleavage of the thioester bond of ~0.4 nm. The latter negative trend indicates that thioester bond lysis requires a structural shortening of the protein conformation, a transition that becomes less favourable as the mechanical load increases.

Our results indicate that thioester bond cleavage is hindered when forces >35 pN are directly applied to the bond and that the kinetics of this reaction are steeply affected by the mechanical load. Methylamine-induced cleavage leads to the covalent binding of this nucleophile to the Gln side-chain, but the backwards reaction involving thioester reformation and ligand uncoupling can occur in the folded state of Cpa. To explore this opposite reaction, we design the force protocol shown in Fig. 4a. After mechanical unfolding of the Cpa polyprotein and the cleavage of the thioester bonds with methylamine (see Fig. 4b), we wash the nucleophile out of the reaction buffer and reduce the force on the protein to favour both the bond reformation and folding of the protein. These conditions allow us to observe a sharp increase in the reformation probability once the Cpa protein is exposed to forces <6 pN (Fig. 4c). The number of reformation events—detected as thioester-intact Cpa unfolding steps at 115 pN—scales with the number of cleavage events observed before the methylamine washout (Extended Data Fig. 1). Interestingly, the bond reformation force range closely tracks that of the folding of thioester-intact Cpa proteins. Given that the Cys and the Gln residues are moved away after cleavage, the force must be decreased to bring close the Cys thiol to attack the Gln carbonyl group and reform the thioester. The fact that Cpa folding occurs at higher forces entails that folding precedes the thioester bond reformation, as it has been also described for the formation of disulfide bonds[33,34].

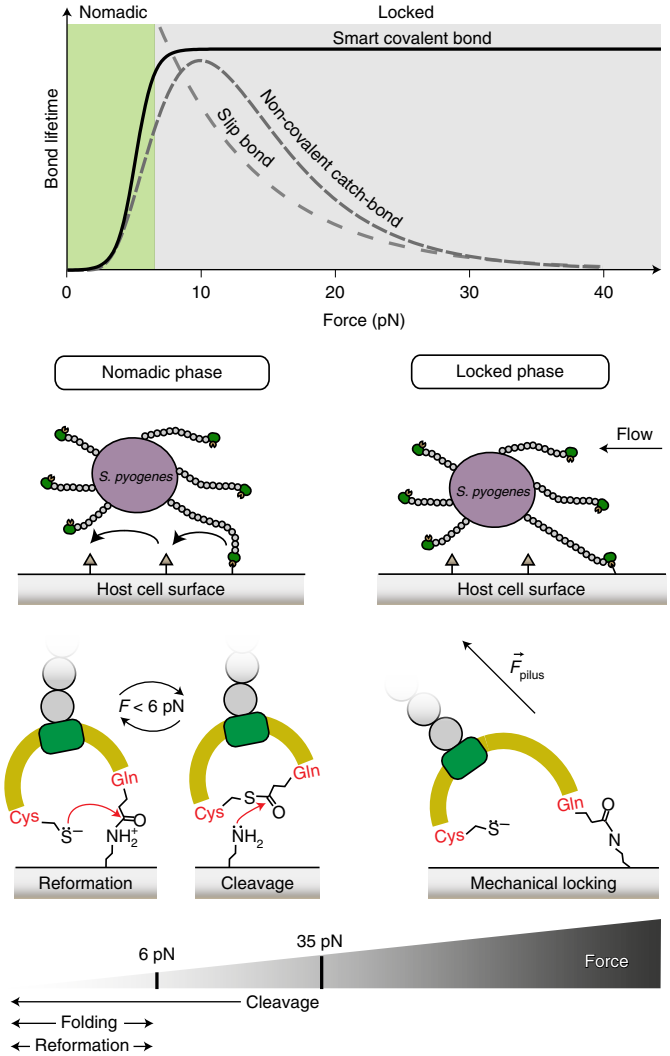


**Fig. 6 | Bacterium mobility strategy model based on the allosteric modulation of the Cpa thioester bond by protein folding.** The graph compares bond lifetimes as a function of the mechanical load for slip bonds, non-covalent catch bonds and smart covalent bonds (slip bond and catch bond data are adapted from ref. [64], plotted in arbitrary units). The smart covalent bond lifetime (plotted as the inverse of the thioester bond reformation probability from Fig. 4c) is defined as the lifetime of the bond made between the surface ligand and the Gln575 side-chain after the nucleophilic cleavage of the thioester bond. Although higher loads exponentially decrease the lifetime of slip bonds, it increases in non-covalent catch bonds; however, loads above a certain threshold decrease the lifetime. The adhesin–ligand smart covalent bond is allosterically modulated by force, establishing short-lived bonds with surface ligands at low mechanical stress—where thioester bond reformation and cleavage coexist—when the protein is folded, but turning into a long-lived bond that permits the bacterium to remain attached under large mechanical challenges, where thioester bond reformation is prevented. We hypothesize that these smart covalent bonds could allow bacteria to switch between a nomadic mobility phase at low force to a mechanically locked phase at larger loads.

**Blocking the thioester bond reformation.** Our experiments with methylamine demonstrate the full reversibility of the cleavage reaction when Cpa is held at low forces and allowed to fold. These experimental conditions resemble the types of interactions that Cpa adhesin could establish with the host ligands, binding and unbinding depending on the mechanical load experienced at the bond interface. From a therapeutic perspective, the irreversible thioester bond cleavage by a ligand analogue would prevent bacterial adhesion, easing the bacterial removal from the tissues by the host's clearance mechanisms—mucus flow, coughing and so on. Taking into account the Cys residue side-chain, we explored the cleavage and reformation of Cpa thioester bond after the treatment with cystamine, another primary-amine nucleophile that contains a disulfide bond in its structure. Following the same protocol as with methylamine, we first unfold thioester-intact Cpa proteins (Fig. 5a, inset histogram 1) and then introduce a solution containing 100 mM cystamine. Following force reduction to 25 and 20 pN for 100 s, the cleavage steps appear, as they did with methylamine (inset histogram 2). After cystamine removal from the solution, the protein is allowed to refold and to reform the thioester bonds at 4 pN. If bond reformation occurs, at 115 pN we should detect the same ~49 nm steps registered before cystamine treatment; however, 97.1 ± 5.2 nm single steps (mean ± s.d., inset histogram 3) appear, which account for the full extension of thioester-cleaved Cpa proteins. Despite attempts to reform the bonds by reducing the force for several cycles (Extended Data Fig. 2), we can only detect full Cpa unfolding steps after cystamine. This nucleophile's disulfide bond can be attacked by Cys426 free thiol to generate an intermolecular disulfide bond (diagram on Fig. 5b). Cys426 thiol oxidation would prevent thioester reformation, which could explain our observations where bond reformation is never observed after cystamine intervention. To further test this hypothesis, we add the reducing agent TCEP to reduce disulfide bonds and liberate the Cys426 thiol. After solution exchange and force reduction, we observe again at high force the unfolding steps of thioester-intact Cpa proteins (Extended Data Fig. 3). Figure 5c compares the cleavage and the reformation probability of the thioester bond after treatment with methylamine and cystamine. Although both nucleophiles exhibit the same cleavage behaviour at 20 and 25 pN, reformation at 4 pN is completely abolished after cystamine treatment; however, if cystamine-blocked proteins are treated with a solution containing 10 mM TCEP, the thioester bond recovery reaches the same values as those with methylamine. Notably, the mechanical resistance of Cpa is considerably reduced when cystamine or methylamine are bound, suggesting a destabilizing role of these molecules on the protein. After the treatment with TCEP, the unfolding kinetics of Cpa are restituted, which indicates that disulfide bond reduction and thioester bond reformation occurred and the cystamine has been expelled from the catalytic pocket of the TED domain (Supplementary Fig. 3). These findings strongly support the idea that cystamine blocking activity relies on the formation of an intermolecular disulfide bond with Cpa Cys426 side-chain, which prevents thioester bond reformation and which can only be rescued after the action of a reducing agent.

## Discussion

Bacterial pathogens possess molecular traits that enable host colonization under mechanical stress. Among these, isopeptide bonds stand out by conferring high mechanical and thermal stability to the adhesive proteins and pili of Gram-positive bacteria[35–37]. These bonds preserve the mechanical integrity of the bacterial anchors[38–40], but ultimately the adhesion lifetime relies on the properties and the strength of the bacteria receptor–host ligand interaction. Gram-positive adhesin–ligand binding has evolved to withstand nanonewton-scale mechanical loads, such as *Staphylococcus epidermidis* SdrG adhesin[41], but also to respond to force in a putative catch bond-like manner, such as *Staphylococcus aureus* ClfA and Clfb adhesins[42,43], or *Streptococcus pneumoniae* pilin RrgB[44]. In the catch bond mechanism, force triggers conformational changes on the adhesin structure that increase the bond lifetime with the ligand, enabling the bacteria to respond to force thresholds[45]. Most of these adhesins interact with extracellular matrix proteins—such

as fibrinogen and collagen[46,47]—and establish non-covalent bonds with their ligands. In addition to these, it was recently discovered the existence of thioester bond-adhesins in some Gram-positive organisms[5–7]. These adhesins can form a covalent bond with the substrate through the nucleophilic attack of its thioester bond by a primary amine ligand, such as the ε-amino group of a Lys residue[5]. Nevertheless, the establishment of an irreversible covalent anchoring would impose a sessile strategy on the cell, hindering its spreading and colonization[48].

Experiments with *S. pyogenes* Cpa adhesin revealed that in the absence of force the thioester bond cleavage by soluble nucleophiles and its reformation existed in equilibrium; however, the application of tensile stress to the thioester bond prevented both its cleavage and reformation, indicating that force modulates the reactivity of this bond[11]. Intramolecular thioester bonds are uncommon in the structure of proteins, having been only identified in the immune complement proteins, in α2-macroglobulin anti-protease[49–51], and in Gram-positive adhesins[6,7]. In the case of non-activated complement proteins, nucleophilic cleavage and reformation can occur[52], but the proteolytic activation of these proteins leads to a rapid and irreversible binding to its target substrates[53], which contrasts with the reversible and force-modulated reactivity of *S. pyogenes* adhesin.

Here, using magnetic tweezers force spectroscopy and a new protocol for the covalent anchoring and assembly of polyproteins, we identify the force range for Cpa thioester bond reactivity. Our results indicate that ligand-induced cleavage occurs when the thioester bond is held at forces <35 pN. This impaired reactivity under force contrasts with the positive effect of force on the mechanochemical cleavage of disulfide bonds by small reducing agents. These disulfide reductions proceed via an $S_N2$ mechanism that experiences a ~0.3–0.4 Å elongation to the transition state[13,14]. On the contrary, enzymatically catalysed disulfide reductions by thioredoxin exhibit a negative force dependency, where the substrate polypeptide must contract under force in order to align with key catalytic residues of the enzyme[15,54,55]. A similar mechanism of polypeptide contraction may underlie the observed force dependency of the Cpa thioester bond, as it can be inferred from the negative distance to the transition state we have observed. At lower forces, where thioester bond cleavage is less hindered, the rate of TED unfolding increases exponentially with force; however, as the load increases, the rate of bond cleavage decreases and the TED unfolding rate is slowed down because of the detrimental effect of force on the cleavage reaction, leading to a negative force dependency. We explain the negative force dependency of thioester cleavage as an autocatalytic mechanism that facilitates the nucleophilic attack, as it has been reported in a close Cpa homologue in *S. pyogenes*[8]; the mechanical load would disrupt the thioester active site and inhibit bond cleavage, deforming the spatial arrangement of key catalytic residues placed in the vicinity of the Cys–Gln bond. Notably, we observe small stepwise fluctuations at forces below 35 pN, which precede thioester cleavage and disappear after the reaction occurs (Supplementary Fig. 4); however, no single discrete step size population is apparent and we cannot assign a specific structural transition to these fluctuations. Nevertheless, the close temporal relationship of these fluctuations to thioester cleavage events suggests a requirement of some structural contraction, and in turn a negative force dependency to the reaction rate. In the backwards reaction, the Cys426 and Gln575 residues must be in close proximity for thioester reformation, which is most probable at or close to the native folded state. Supporting this mechanism, we measured the folding force dependency of thioester-intact Cpa (Fig. 2c), which closely tracks the profile of thioester reformation (Fig. 4c). This pathway of refolding followed by reformation can explain the sharp transition in the force dependency from 4 pN to 6 pN, with reformation restricted to the force range of protein folding. This behaviour shows an analogy with the process of enzymatic-assisted oxidative folding, where protein folding brings in close proximity the Cys residues involved before disulfide bond formation can proceed[33,56].

Importantly, our experimental pulling axis from the N and C ends of Cpa is not the physiological one. In our system, the introduction of the D595A mutation abrogates the formation of the native isopeptide bond present in the CnaB domain of Cpa, which in the native protein shields the TED domain from experiencing force when pulled from the N and the C termini. This pulling configuration has enabled us to explore in real time the thioester bond dynamics in the presence of nucleophiles with unprecedented resolution. Although the thioester bond in the native folded TED domain is not expected to be under tensile stress, we can expect that its in vivo reactivity will be modulated by force. In our previous work, the simulation of the in vivo pulling axis between the C-terminus residue—connected to the pilus—and Gln575—linked to the surface ligand—revealed mechanical deformation of the thioester active site[11], suggesting that the TED domain experiences force on surface ligand-induced cleavage of the thioester bond and binding to the Gln575 side-chain. This mechanical deformation would alter the position of key residues involved in the thioester bond reactivity, hindering the reformation process and extending the lifetime of the adhesin–ligand bond. This in vivo geometry indicates that thioester bond reformation is affected by force and, although we cannot access experimentally the exact force pathway, the force dependency of reformation is not expected to be dependent on the pulling axis. The effect of different pulling geometries on the unfolding of proteins has been widely explored in the force spectroscopy field and, whereas the specific unfolding forces can change depending on how the force is applied, the force dependency of this reaction remains unaltered[57–60]. In the case of the Cpa adhesin, although the native pulling configuration would probably affect quantitatively the force range at which reformation occurs, our approach clearly identifies and underpins the force-dependent modulation of this bond. Based on our observations, we hypothesize that the bond reactivity modulation by folding could have implications in the bacterium adhesion strategy, reconciling the mobility and the anchoring problem (Fig. 6). Non-covalent catch bonds show an increased lifetime at certain levels of mechanical load, but exceeding forces terminate the binding[45]. In the absence of force, thioester bonds would operate as catch bonds, where surface ligands cleave them but reformation can occur, as long as the protein remains in the unperturbed folded state. Under these conditions, soluble ligands such as histamine—which is released at infection sites[61]—can also bind to Cpa and compete with the surface targets of the adhesin. However, the lack of tensile stress in the Gln575–histamine interface would allow the Cys–Gln thioester bond reformation, which would release the histamine and reset Cpa ready for another incoming ligand. By contrast, increasing mechanical loads on those bonds established with surface-bound ligands at low force would prevent reformation due to the mechanical deformation and partial unfolding of Cpa—mechanical allostery—inducing a long-lived covalent bond able to survive nanonewton-scale perturbations[62,63]. Only after the mechanical challenge is finished and the force is reduced can Cpa folding and bond reformation occur to favour cell rolling again. Given the folding-modulated reactivity of this adhesin thioester bond, and its possible implications for Gram-positive adhesion, we dub these adhesin–ligand interactions as smart covalent bonds. This mechanism could provide the bacterium with a balanced strategy: to switch from a nomadic phase at low shear stress that optimizes cell spreading (cleavage-binding and reformation-unbinding states coexist), to a locked phase under harsh mechanical conditions that induce dislodgement (bound state). The demonstration of the existence of such a mechanism would add another adhesion strategy class to the repertoire observed in bacterial attachment.

Our results indicate that protein folding can modulate the binding activity of *S. pyogenes* Cpa, and they also indicate that

chemically targeting the Cys–Gln thioester bond can be of potential interest for the development of antiadhesive drugs. The inhibitory effect observed after the treatment with cystamine indicates that, after nucleophilic cleavage, disulfide bond exchange occurs between Cys426 free thiol and cystamine disulfide bond, arresting the reformation. This conclusion is supported by the regenerative effect registered after TCEP treatment, which reduces the cystamine–Cpa intermolecular disulfide bond and frees the Cys426 thiol, enabling the reformation reaction. Although methylamine and histamine transiently cleave the thioester bond, bifunctional soluble ligands with nucleophilic and thiol oxidation activities could permanently bind to Cpa to disable its adhesin function, establishing a new therapeutic path to tackle the antibiotic resistance problem.

## Online content

Any methods, additional references, Nature Research reporting summaries, source data, extended data, supplementary information, acknowledgements, peer review information; details of author contributions and competing interests; and statements of data and code availability are available at https://doi.org/10.1038/s41557-020-00586-x.

Received: 21 August 2019; Accepted: 29 September 2020;
Published online: 30 November 2020

## References

1. Hall-Stoodley, L., Costerton, J. W. & Stoodley, P. Bacterial biofilms: from the natural environment to infectious diseases. *Nat. Rev. Microbiol.* **2**, 95–108 (2004).
2. Yan, J. & Bassler, B. L. Surviving as a community: antibiotic tolerance and persistence in bacterial biofilms. *Cell Host Microbe* **26**, 15–21 (2019).
3. Forero, M., Yakovenko, O., Sokurenko, E. V., Thomas, W. E. & Vogel, V. Uncoiling mechanics of *Escherichia coli* type I fimbriae are optimized for catch bonds. *PLoS Biol.* **4**, 1509–1516 (2006).
4. Sauer, M. M. et al. Catch-bond mechanism of the bacterial adhesin FimH. *Nat. Commun.* **7**, 10738 (2016).
5. Pointon, J. A. et al. A highly unusual thioester bond in a pilus adhesin is required for efficient host cell interaction. *J. Biol. Chem.* **285**, 33858–33866 (2010).
6. Walden, M. et al. An internal thioester in a pathogen surface protein mediates covalent host binding. *Elife* **4**, 1–24 (2015).
7. Miller, O. K., Banfield, M. J. & Schwarz-Linek, U. A new structural class of bacterial thioester domains reveals a slipknot topology. *Protein Sci.* **22**, 1–50 (2018).
8. Linke-Winnebeck, C. et al. Structural model for covalent adhesion of the *Streptococcus pyogenes* pilus through a thioester bond. *J. Biol. Chem.* **289**, 177–189 (2014).
9. Anderson, B. N. et al. Weak rolling adhesion enhances bacterial surface colonization. *J. Bacteriol.* **189**, 1794–1802 (2007).
10. Marshall, K. C. in *The Prokaryotes* 191–201 (Springer, 2013); https://doi.org/10.1007/978-3-642-30123-0_49
11. Echelman, D. J., Lee, A. Q. & Fernández, J. M. Mechanical forces regulate the reactivity of a thioester bond in a bacterial adhesin. *J. Biol. Chem.* **292**, 8988–8997 (2017).
12. Brouwer, S., Barnett, T. C., Rivera-Hernandez, T., Rohde, M. & Walker, M. J. *Streptococcus pyogenes* adhesion and colonization. *FEBS Lett.* **590**, 3739–3757 (2016).
13. Koti Ainavarapu, S. R., Wiita, A. P., Dougan, L., Uggerud, E. & Fernandez, J. M. Single-molecule force spectroscopy measurements of bond elongation during a bimolecular reaction. *J. Am. Chem. Soc.* **130**, 6479–6487 (2008).
14. Wiita, A. P., Ainavarapu, S. R. K., Huang, H. H. & Fernandez, J. M. Force-dependent chemical kinetics of disulfide bond reduction observed with single-molecule techniques. *Proc. Natl Acad. Sci. USA* **103**, 7222–7227 (2006).
15. Wiita, A. P. et al. Probing the chemistry of thioredoxin catalysis with force. *Nature* **450**, 124–127 (2007).
16. Schönfelder, J., De Sancho, D. & Perez-Jimenez, R. The power of force: insights into the protein folding process using single-molecule force spectroscopy. *J. Mol. Biol.* **428**, 4245–4257 (2016).
17. Popa, I. et al. A halotag anchored ruler for week-long studies of protein dynamics. *J. Am. Chem. Soc.* **138**, 10546–10553 (2016).
18. Tapia-Rojo, R., Eckels, E. C. & Fernández, J. M. Ephemeral states in protein folding under force captured with a magnetic tweezers design. *Proc. Natl Acad. Sci. USA* **116**, 7873–7878 (2019).
19. Taniguchi, Y. & Kawakami, M. Application of Halotag protein to covalent immobilization of recombinant proteins for single molecule force spectroscopy. *Langmuir* **26**, 10433–10436 (2010).
20. Popa, I. et al. Nanomechanics of halotag tethers. *J. Am. Chem. Soc.* **135**, 12762–12771 (2013).
21. Zakeri, B. et al. Peptide tag forming a rapid covalent bond to a protein, through engineering a bacterial adhesin. *Proc. Natl Acad. Sci. USA* **109**, E690–E697 (2012).
22. Janissen, R. et al. Invincible DNA tethers: covalent DNA anchoring for enhanced temporal and force stability in magnetic tweezers experiments. *Nucl. Acids Res.* **42**, e137 (2014).
23. Brujić, J., Hermans, R. I. Z., Garcia-Manyes, S., Walther, K. A. & Fernandez, J. M. Dwell-time distribution analysis of polyprotein unfolding using force-clamp spectroscopy. *Biophys. J.* **92**, 2896–2903 (2007).
24. Durner, E., Ott, W., Nash, M. A. & Gaub, H. E. Post-translational sortase-mediated attachment of high-strength force spectroscopy handles. *ACS Omega* **2**, 3064–3069 (2017).
25. Deng, Y. et al. Enzymatic biosynthesis and immobilization of polyprotein verified at the single-molecule level. *Nat. Commun.* **10**, 2775 (2019).
26. *Antibiotic Resistance Threats in the United States, 2013* (CDC, 2013).
27. Cascioferro, S., Cusimano, M. G. & Schillaci, D. Antiadhesion agents against Gram-positive pathogens. *Future Microbiol.* **9**, 1209–1220 (2014).
28. *The Bacterial Challenge: Time to React* (ECDC, EMA 2009).
29. Veggiani, G. et al. Programmable polyproteams built using twin peptide superglues. *Proc. Natl Acad. Sci. USA* **113**, 1202–1207 (2016).
30. Min, D., Arbing, M. A., Jefferson, R. E. & Bowie, J. U. A simple DNA handle attachment method for single molecule mechanical manipulation experiments. *Protein Sci.* **25**, 1535–1544 (2016).
31. Flory, P. J. Theory of elastic mechanisms in fibrous proteins. *J. Am. Chem. Soc.* **78**, 5222–5235 (1956).
32. Bell, G. Models for the specific adhesion of cells to cells. *Science* **200**, 618–627 (1978).
33. Kosuri, P. et al. Protein folding drives disulfide formation. *Cell* **151**, 794–806 (2012).
34. Eckels, E. C., Haldar, S., Tapia-Rojo, R., Rivas-Pardo, J. A. & Fernández, J. M. The mechanical power of titin folding. *Cell Rep* **27**, 1836–1847.e4 (2019).
35. Kang, H. J. & Baker, E. N. Intramolecular isopeptide bonds give thermodynamic and proteolytic stability to the major pilin protein of *Streptococcus pyogenes*. *J. Biol. Chem.* **284**, 20729–20737 (2009).
36. Alegre-Cebollada, J., Badilla, C. L. & Fernández, J. M. Isopeptide bonds block the mechanical extension of pili in pathogenic *Streptococcus pyogenes*. *J. Biol. Chem.* **285**, 11235–11242 (2010).
37. Echelman, D. J. et al. CnaA domains in bacterial pili are efficient dissipaters of large mechanical shocks. *Proc. Natl Acad. Sci. USA* **113**, 2490–2495 (2016).
38. Rivas-Pardo, J. A., Badilla, C. L., Tapia-Rojo, R., Alonso-Caballero, Á. & Fernández, J. M. Molecular strategy for blocking isopeptide bond formation in nascent pilin proteins. *Proc. Natl Acad. Sci. USA* **115**, 9222–9227 (2018).
39. Wang, B., Xiao, S., Edwards, S. A. & Gräter, F. Isopeptide bonds mechanically stabilize Spy0128 in bacterial pili. *Biophys. J.* **104**, 2051–2057 (2013).
40. Kang, H. J. & Baker, E. N. Intramolecular isopeptide bonds: protein crosslinks built for stress? *Trends Biochem. Sci.* **36**, 229–237 (2011).
41. Milles, L. F., Schulten, K., Gaub, H. E. & Bernardi, R. C. Molecular mechanism of extreme mechanostability in a pathogen adhesin. *Science (80-.)* **359**, 1527–1533 (2018).
42. Herman-Bausier, P. et al. *Staphylococcus aureus* clumping factor A is a force-sensitive molecular switch that activates bacterial adhesion. *Proc. Natl Acad. Sci. USA* **115**, 5564–5569 (2018).
43. Vitry, P. et al. Force-induced strengthening of the interaction between *Staphylococcus aureus* clumping factor B and loricrin. *MBio* **8**, 1–14 (2017).
44. Becke, T. D. et al. Pilus-1 backbone protein RrgB of streptococcus pneumoniae binds Collagen I in a force-dependent way. *ACS Nano* **13**, 7155–7165 (2019).
45. Thomas, W. E., Vogel, V. & Sokurenko, E. Biophysics of catch bonds. *Annu. Rev. Biophys.* **37**, 399–416 (2008).
46. Sridharan, U. & Ponnuraj, K. Isopeptide bond in collagen- and fibrinogen-binding MSCRAMMs. *Biophys. Rev.* **8**, 75–83 (2016).
47. Kreikemeyer, B. et al. *Streptococcus pyogenes* collagen type I-binding Cpa surface protein: expression profile, binding characteristics, biological functions, and potential clinical impact. *J. Biol. Chem.* **280**, 33228–33239 (2005).
48. Stewart, P. S. Biophysics of biofilm infection. *Pathog. Dis.* **70**, 212–218 (2014).
49. Law, S. K. & Dodds, A. W. The internal thioester and the covalent binding properties of the complement proteins C3 and C4. *Protein Sci.* **6**, 263–274 (1997).
50. Garcia-Ferrer, I. et al. Structural and functional insights into *Escherichia coli* α2-macroglobulin endopeptidase snap-trap inhibition. *Proc. Natl Acad. Sci. USA* **112**, 8290–8295 (2015).
51. Wong, S. G. & Dessen, A. Structure of a bacterial α2-macroglobulin reveals mimicry of eukaryotic innate immunity. *Nat. Commun.* **5**, 4917 (2014).

52. Dodds, A. W., Ren, X.-D., Willis, A. C. & Law, S. K. A. The reaction mechanism of the internal thioester in the human complement component C4. *Nature* **379**, 177–179 (1996).
53. Nilsson, B. & Nilsson Ekdahl, K. The tick-over theory revisited: is C3 a contact-activated protein? *Immunobiology* **217**, 1106–1110 (2012).
54. Alegre-Cebollada, J., Perez-Jimenez, R., Kosuri, P. & Fernandez, J. M. Single-molecule force spectroscopy approach to enzyme catalysis. *J. Biol. Chem.* **285**, 18961–18966 (2010).
55. Liang, J. & Fernández, J. M. Mechanochemistry: one bond at a time. *ACS Nano* **3**, 1628–1645 (2009).
56. Kahn, T. B., Fernández, J. M. & Perez-Jimenez, R. Monitoring oxidative folding of a single protein catalyzed by the disulfide oxidoreductase DsbA. *J. Biol. Chem.* **290**, 14518–14527 (2015).
57. Carrion-Vazquez, M. et al. The mechanical stability of ubiquitin is linkage dependent. *Nat. Struct. Biol.* **10**, 738–743 (2003).
58. Jagannathan, B., Elms, P. J., Bustamante, C. & Marqusee, S. Direct observation of a force-induced switch in the anisotropic mechanical unfolding pathway of a protein. *Proc. Natl Acad. Sci. USA* **109**, 17820–17825 (2012).
59. Dietz, H., Berkemeier, F., Bertz, M. & Rief, M. Anisotropic deformation response of single protein molecules. *Proc. Natl Acad. Sci. USA* **103**, 12724–12728 (2006).
60. Brockwell, D. J. et al. Pulling geometry defines the mechanical resistance of a β-sheet protein. *Nat. Struct. Biol.* **10**, 731–737 (2003).
61. Stone, K. D., Prussin, C. & Metcalfe, D. D. IgE, mast cells, basophils, and eosinophils. *J. Allergy Clin. Immunol.* **125**, S73–S80 (2010).
62. Grandbois, M., Beyer, M., Rief, M., Clausen-Schaumann, H. & Gaub, H. E. How strong is a covalent bond. *Science* **283**, 1727–1730 (1999).
63. Pill, M. F., East, A. L. L., Marx, D., Beyer, M. K. & Clausen-Schaumann, H. Mechanical activation drastically accelerates amide bond hydrolysis, matching enzyme activity. *Angew. Chem. Int. Ed.* **58**, 9787–9790 (2019).
64. Marshall, BryanT. et al. Direct observation of catch bonds involving cell-adhesion molecules. *Nature* **423**, 190–193 (2003).

## Methods

**Protein engineering and expression.** All the reagents employed in this research were from Sigma–Aldrich, unless otherwise specified. The *S. pyogenes* Cpa gene was kindly provided by M. Banfield (John Innes Centre). The gene was modified to include a 5'-end BamHI restriction site, a point mutation D595A to abolish CnaB(M) intramolecular isopeptide bond formation, and 3'-end BglII and KpnI restriction sites, as described previously in ref. [11]. A polyprotein containing four copies of Cpa—CnaB(M)–TED(T)—was assembled through successive cloning steps involving BamHI, BglII and KpnI restriction sites, using pT7Blue (Novagen) as the cloning plasmid. The construct was then digested with BamHI/BglII and cloned into the expression plasmid pQE80L (Qiagen), which carries a N-terminal His tag. This plasmid was previously modified to contain two copies of the SpyTag sequence with a BamHI restriction site in between, which was digested to allow the insertion of the construct, generating the SpyTag-$(Cpa)_4$–SpyTag construct (pQE80L–SpyTag–$(CnaB_{D595A})_4$–SpyTag). All of the cloning and amplification steps were performed in XL10-Gold *Escherichia coli* (*E. Coli*) cells (Agilent Technologies). The probe and surface anchor protein, SpyCatcher–HaloTag, was cloned using this same protocol of digestion and ligation of restriction enzyme sites, and finally transferred to an empty pQE80L expression plasmid (pQE80L–SpyCatcher–HaloTag). The C-terminal HaloTag protein version was used for this construct[20].

Protein expression and purification was done as described elsewhere[36]. In brief, *E. coli* ERL cells (kindly provided by R.T. Sauer from the Massachusetts Institute of Technology) were transformed with the pQE80L–SpyTag–$(Cpa)_4$–SpyTag plasmid or pQE80L–SpyCatcher–HaloTag, and protein expression was induced with 1 mM Isopropyl β-D-1-thiogalactopyranoside overnight at 25 °C or 37 °C, respectively. Cells were lysed in a French press (Sim-Aminco) and then the proteins were purified from the lysate with the His60 Ni Superflow Resin (Clontech). An additional purification step was performed through size-exclusion chromatography in a Superdex 200 FPLC column (GE Healthcare), eluting the proteins in 10 mM Hepes (pH 7.2), 150 mM NaCl, 1 mM EDTA (Hepes buffer). In the case of SpyCatcher–HaloTag protein, Hepes buffer further contained 10% v/v of glycerol. Purified proteins were aliquoted and frozen at −20 °C until their use.

**Cpa protein sequence.** The $Cpa_{D595A}$ sequence is presented below. The sequence of the CnaB domain is highlighted in bold. The sequence of the TED domain, which spans from A393 to G579, is in italics. C426 and Q575, the residues which form the thioester bond between their side chains, are in italic and underlined. The residue A595, which is a mutation from the native D595 residue, is bold and underlined.

**NQPQTTSVLIRKYAIGDYSKLLEGATLQLTGDNVNSFQARVFSSNDIGE-RIELSDGTYTLTELNSPAGYSIAEPITFKVEAGKVYTIIDGKQIENPNKEIV-EPYSVE***AYNDFEEFSVLTTQNYAKFYYAKNKNGSSQVVYCFNADLKSPPDSE-DGGKTMTPDFTTGEVKYTHIAGRDLFKYTVKPRDTDPDTFLKHIKKVIEKGY REKGQAIEYSGLTETQLRAATQLAIYYFTDSAELDKDKLKDYHGFGDMNDSTLAVAKILVEY AQDSNPPQLTDLDFFIPNNNKYQSLIG***TQWHPEDLVDIIRMEAKKEV**

**Bead surface functionalization.** We washed $10^8$ amine-coated Dynabeads M270 (Thermo Fisher Scientific) in PBS buffer (pH 7.4) and incubated them in a PBS solution containing 1% v/v glutaraldehyde for 1 h in a rotator at 18 r.p.m. (Labnet). After extensive washing, the beads were incubated in a PBS solution containing 25 μg ml$^{-1}$ of the HaloTag ligand O4 (Promega) for at least 4 h at constant rotation. After washing, beads were treated with blocking buffer, which contains Tris-HCl pH 7.4, NaCl 150 mM, $NaN_3$ 0.001% w/v and 1% w/v of sulfhydryl-blocked bovine serum albumin (Lee Biosolutions) overnight at 4 °C and at constant rotation. Optimal bead protein functionalization was achieved with a 15:5 μM ratio of HaloTag protein to SpyCatcher–HaloTag for at least 12 h at 4 °C and constant rotation. This 3:1 molar ratio results in an optimal bead surface coverage that prevents the formation of multiple tethers, since only the SpyCatcher–HaloTag molecules will serve as anchors for the glass surface-bound proteins. Beads were stored under this condition until use, moment in which they were extensively washed to remove unbound protein.

**Fluid chamber functionalization.** Magnetic tweezers experiments were conducted on fluid chambers made of two sandwiched glasses (Ted Pella) of 24 × 40 mm (bottom) and 22 × 22 (top), which were separated by a thin parafilm template cut with a laser cutting machine (Superland). The templates have a bow-tie-like shape that allows the immobilization of the top glass over the bottom glass and the formation of one well on each end of the bottom glass, which permits the exchange of buffer along the experiments. Before fluid chamber assembly, bottom glasses were washed and sonicated for 20 min in Hellmanex 1% (Helma), acetone and ethanol. After the wash, the glasses were dried and exposed to air plasma for 15 min. Glasses were then silanized for 20 min with an ethanol solution containing 0.1% v/v of (3-aminopropyl)-trimethoxysilane, followed by several washes in ethanol. Finally, the glasses were dried with air, baked at 100 °C for more than 20 min and stored in a desiccator until further use. Top glasses were sonicated for 20 min in Hellmanex 1%, washed with ethanol, dried with air and dried at 100 °C for 10 min. The top glasses were then placed inside of a glass beaker and immersed in repel silane (Sigma) for 30 min at room temperature to make them hydrophobic. The glasses were then dried with air, baked for 20 min at 100 °C and stored in a desiccator until use.

Fluid chambers assembly was done sandwiching the parafilm bow-tie templates between the bottom and the top glasses, placed over a hot plate at 85 °C, and with a flat 1 kg aluminium block pressing it. After 10 min, the fluid chambers were removed from the plate and a solution of PBS pH 7.4 with glutaraldehyde 1% v/v was flowed into the chambers and left to react for 1 h. A PBS solution containing 0.02% w/v of 3.5–3.9 μm amine-coated polystyrene beads (Spherotech) was then flowed and incubated for 20 min. After washing extensively, a PBS solution containing 25 μg ml$^{-1}$ of the HaloTag ligand O4 was incubated overnight at room temperature. Finally, the fluid chambers were washed, blocked with blocking buffer overnight at room temperature, and stored at 4 °C until further use.

**Double-covalent and molecular assembly.** Fluid chambers were incubated with 5 μM SpyCatcher–HaloTag for 30 min. After an extensive rinse with Hepes buffer, the chambers were incubated with 5 μM SpyTag–(CnaB–TED)4-SpyTag for at least 1 h, and then extensively rinsed again. Once the fluid chamber was placed on the microscope, 20 μl of a 1:10 dilution of HaloTag:SpyCatcher–HaloTag-functionalized beads were added to the fluid chamber and recirculated twice. Beads were then allowed to react with the surface-bound molecules for 5 min before approaching the magnets and starting the experiment.

**Magnetic tweezers force spectroscopy.** Force spectroscopy experiments were conducted on a custom-built magnetic tweezers apparatus, as previously described[17]. The experimental fluid chambers were placed on the top of an inverted microscope (Olympus IX-71/Zeiss Axiovert S100) and illuminated with a collimated cold white light-emitting diode (ThorLabs). The reference beads and the protein-bound paramagnetic beads were visualized employing a 100× oil-immersion objective (Zeiss/Olympus), which was mounted on a nanofocusing piezo actuator (P-725; Physik Instrumente). Image acquisition was performed using a CMOS Ximea MQ013MG-ON camera, and image processing was performed with custom-written C++/Qt software[65]. Data acquisition and piezo position control were performed using a multifunction DAQ card (NI USB-6289, National Instruments). Proteins were exposed to calibrated forces using a pair of magnets mounted on the top of a voice-coil (Equipment Solutions) placed above the experimental fluid chamber. The positions of the magnets were maintained under electronic feedback using a proportional–integral–derivative controller.

**Single-molecule magnetic tweezers experiments on thioester bond cleavage and reformation.** All of the experiments were commenced by applying a force of 4 pN, which lifts the protein-bound beads from the surface and prevents nonspecific interactions. The unfolding pulses were done at 115 pN, until the complete unfolding of the thioester-intact Cpa domains (~49 nm steps). Only molecules showing the initial unfolding of 3 or 4 domains were considered. Buffer exchange to add or remove nucleophile molecules was performed at 115 pN. On nucleophile addition to the fluid chamber, thioester bond cleavage was monitored on 100 s time windows at forces ranging from 10 to 35 pN. A 115 pN pulse was then applied to monitor and compare the final extension of the molecule before and after the nucleophile treatment. At this high force, the nucleophile-containing buffer was washed out and then the force was quenched for 100 s at forces ranging from 3 to 7 pN, to favour refolding and thioester bond reformation. The folding and the thioester bond status of the domains were subsequently evaluated with a 115 pN pulse. In the case of folding and thioester bond reformation, thioester-intact Cpa domains were detected (~49 nm steps); in the case of having only folding, the full extension of the Cpa domain was observed (~95 nm steps). The buffer used along the experiments contained 50 mM Hepes pH 8.5, 150 mM NaCl, 1 mM EDTA, 10 mM L-ascorbic acid (to prevent oxidative damage[66]), and was supplemented with 100 mM of methylamine or cystamine for the thioester bond cleavage. To induce thioester bond reformation after cystamine treatment, the same buffer but supplemented with 10 mM of TCEP was added and the force quenched to 4 pN to favour folding and reformation. At least three different molecules were used for each data point collected.

**Analysis.** Analysis was performed with Igor Pro 8.0 software (Wavemetrics)[65]. Recordings were smoothed using a fourth-order Savitzky–Golay filter with a box size of 51 points. Step sizes were determined measuring the distance between the peaks of Gaussian fits performed on the unfolding steps. The folding probability was calculated as the ratio between the number of unfolded domains and the number of domains able to fold after 100 s at each of the forces tested. The thioester bond cleavage probability on 100 s time windows was calculated as the ratio between detected cleavage steps at any of the forces tested, and the number of thioester-intact Cpa domains susceptible to cleaving. Reformation probability was calculated as the ratio between thioester-intact Cpa domains detected and the number of cleaved domains registered before. For folding, cleavage and reformation probabilities, a jackknife estimator was used for the calculation of the average probability and the s.d.

**Thioester bond cleavage kinetics.** In Fig. 3c we show the kinetics of thioester bond-cleavage/TED domain unfolding under force in the presence of methylamine. In these experiments, we detect the unfolding of the previously trapped sequence of the TED domain by the thioester bond along unrestricted time windows.

Direct observation of thioester bond cleavage before unfolding was not possible under these experimental conditions as the cleavage does not produce an extension signature that is detectable by our technique. Between 10 and 20 pN, the force reduces the time to detect the mechanical extension of the TED domain. On the contrary, this process slowed down between 20 and 30 pN, and TED domain extension requires longer exposure times as the force is increased. We rationalize this change in the kinetics of this process under force as the result of two sequential processes with opposite force dependencies. At forces <20 pN, cleavage of the bond occurs, but the mechanical unfolding of the TED domain becomes limiting, increasing the waiting time for the detection of its unfolding step. At forces >20 pN, the mechanical unfolding of the TED domain was increasingly favoured, but the negative effect of the force on the thioester bond geometry and the neighbouring residues of the catalytic pocket of the protein impairs the nucleophilic attack by methylamine, resulting in slower kinetics of TED domain extension.

This picture can be formalized as a two-step kinetic process. Schematically, it can be represented as:

$$\mathrm{TED} \xrightarrow{k_C} \mathrm{TED}^{*} \xrightarrow{k_U} \mathrm{TED}^{*}_{U}$$

where TED is the folded and bonded TED state, TED$^{*}$ the folded and cleaved TED state, and TED$^{*}_{U}$ the cleaved and unfolded TED state. The thioester bond cleavage process ($k_C$) must occur before TED domain unfolding ($k_U$) can be detected. Here we assume that the rates of folding ($k_F$) and bond reformation ($k_R$) are negligible in the force range tested, as Fig. 4c suggests. As we cannot observe the transition from TED to TED$^{*}$ ($k_C$), what we observe is the transition ($k_{obs}$) from the initial to the final state (TED to TED$^{*}_{U}$):

$$\mathrm{TED} \xrightarrow{k_{obs}} \mathrm{TED}^{*}_{U}, \text{ where we observe : } \frac{d\mathrm{TED}^{*}_{U}}{dt}$$

These assumptions lead to the next set of linear differential equations:

$$\frac{dP_{\mathrm{TED}}}{dt} = -k_C P_{\mathrm{TED}},$$

$$\frac{dP_{\mathrm{TED}^{*}}}{dt} = k_C P_{\mathrm{TED}} - k_U P_{\mathrm{TED}^{*}}, \quad (1)$$

$$\frac{dP_{\mathrm{TED}^{*}_{U}}}{dt} = k_U P_{\mathrm{TED}^{*}},$$

which have:

$$P_{\mathrm{TED}} + P_{\mathrm{TED}^{*}} + P_{\mathrm{TED}^{*}_{U}} = 1$$

as a boundary condition, and these initial conditions:

$$P_{\mathrm{TED}}(0) = 1; P_{\mathrm{TED}^{*}}(0) = 0; P_{\mathrm{TED}^{*}_{U}}(0) = 0$$

where, $P_{\mathrm{TED}}$, $P_{\mathrm{TED}^{*}}$ and $P_{\mathrm{TEDu}^{*}}$ are the occupation probabilities of the folded and bonded TED state, the folded and cleaved TED state, and the cleaved and unfolded TED state, respectively. In our experiments, we measure the time ($t_{obs}$) required to reach the cleaved and unfolded state (TED$^{*}_{U}$), and we calculate the observed rate as:

$$k_{obs} = \frac{1}{\langle t_{obs} \rangle}; \langle t_{obs} \rangle = \int_0^{\infty} t f(t)\, dt; \text{ with} f(t) = \frac{dP_{\mathrm{TED}^{*}_{U}}}{dt},$$

Where $\langle t_{obs} \rangle$ is the average time. Hence, from this expression we can calculate $k_{obs}$, which contains $k_C$ and $k_U$.

$$k_{obs} = \frac{k_C k_U}{k_C + k_U} \quad (2)$$

Assuming the Bell model for bond lifetimes[32], we use an expression that accounts for both opposing processes and explains the tendency we report in this study:

$$k_C(F) = k_C^0 e^{\frac{-x_C^{\dagger} F}{k_B T}} \text{ and } k_U(F) = k_U^0 e^{\frac{x_U^{\dagger} F}{k_B T}}$$

Where $k_C$ is the rate of thioester bond cleavage as a function of force ($F$), $k_C^0$ is the rate of thioester bond cleavage in the absence of force, $-x_C^{\dagger}$ is the negative distance to the transition state, $F$ is the force, $k_B$ is the Boltzmann constant and $T$ is the temperature. In the case of unfolding, $k_U$ is the rate of TED unfolding as a function of force, $k_U^0$ is the rate of protein unfolding in the absence of force, and $x_U^{\dagger}$ is the distance to the transition state. Finally, the expression used to fit the data in Fig. 3c is:

$$k_{obs} = \frac{k_C^0 e^{\frac{-x_C^{\dagger} F}{k_B T}} k_U^0 e^{\frac{x_U^{\dagger} F}{k_B T}}}{k_C^0 e^{\frac{-x_C^{\dagger} F}{k_B T}} + k_U^0 e^{\frac{x_U^{\dagger} F}{k_B T}}} \quad (3)$$

From this fit, we obtain $k_C^0 = 0.32 \pm 0.26\,s^{-1}$ and $x_C^{\dagger} = -0.41 \pm 0.26$ nm and $k_U^0 = (2.94 \pm 3.58) \times 10^{-3}\,s^{-1}$ and $x_U^{\dagger} = 0.94 \pm 0.51$ nm. The dotted lines showed in Fig. 3c correspond to the individual rates $k_C(F)$ and $k_U(F)$ as obtained from the fit to equation (3).

## Data availability

All data supporting the results and conclusions are available within this paper and the Supplementary Information. Source data are provided with this paper.

## References

65. Tapia-Rojo, R., Alonso-Caballero, A. & Fernandez, J. M. Direct observation of a coil-to-helix contraction triggered by vinculin binding to talin. *Sci. Adv.* **6**, eaaz4707 (2020).
66. Valle-Orero, J. et al. Mechanical deformation accelerates protein ageing. *Angew. Chem. Int. Ed.* **56**, 9741–9746 (2017).

## Acknowledgements

This research was supported by the National Institutes of Health grant no. R35129962 (J.M.F). A.A-C. and R.T-R. express their gratitude to Fundación Ramón Areces (Madrid, Spain) for financial support. We thank C. L. Badilla for assistance in molecular biology procedures, and for reading and reviewing the manuscript. Correspondence and request for materials should be addressed to A.A-C

## Author contributions

D.J.E., A.A-C. and J.M.F designed the research. A.A-C, D.J.E., R.T-R., S.H., E.C.E carried out the experiments. A.A-C, D.J.E., R.T-R. analysed the data. A.A-C., D.J.E., and J.M.F. wrote the manuscript.

## Competing interests

The authors declare no competing interests.

## Additional information

**Extended data** is available for this paper at https://doi.org/10.1038/s41557-020-00586-x.

**Supplementary information** is available for this paper at https://doi.org/10.1038/s41557-020-00586-x.

**Correspondence and requests for materials** should be addressed to A.A.-C.

**Reprints and permissions information** is available at www.nature.com/reprints.

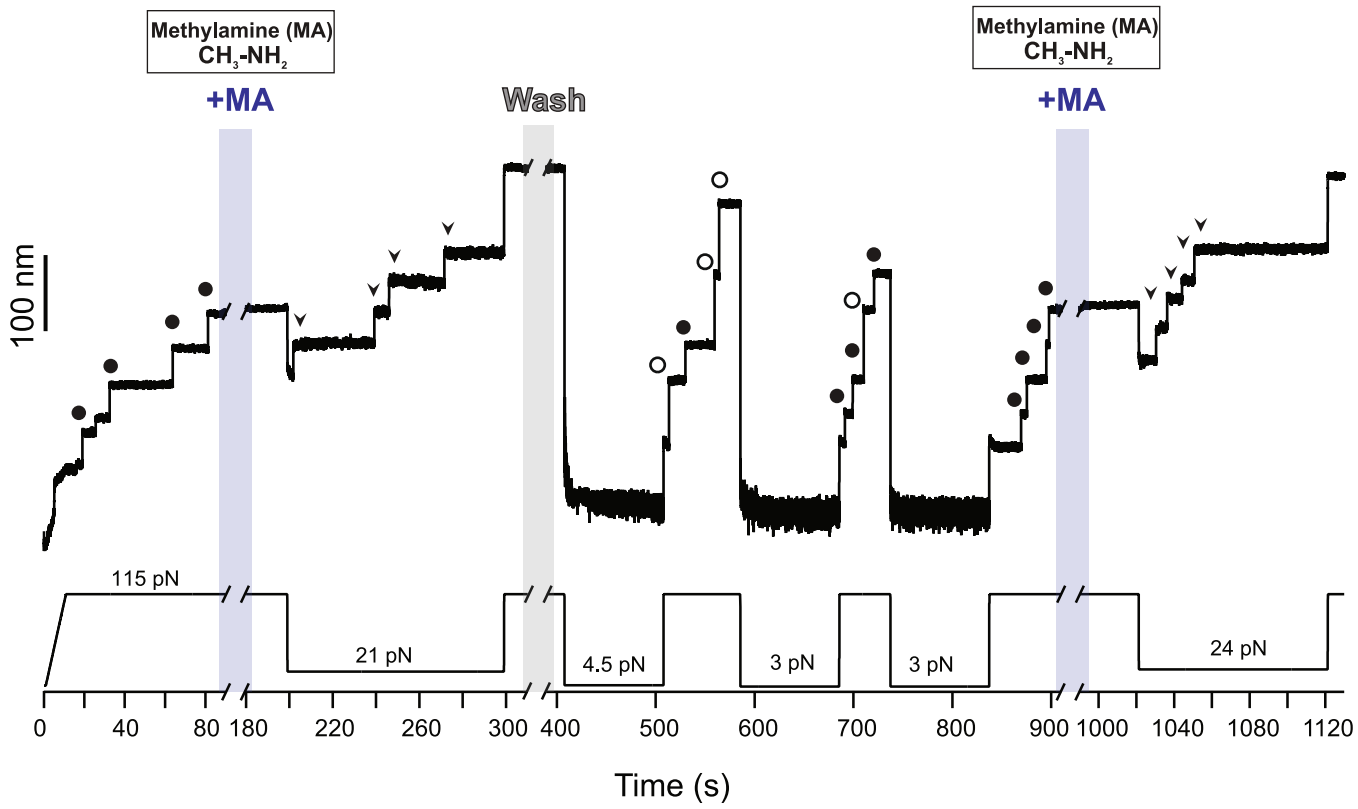


**Extended Data Fig. 1 | Cleavage-reformation-cleavage sequence.** Magnetic tweezers force-clamp trajectory of the Cpa polyprotein. After the unfolding of four thioester-intact Cpa domains at 115 pN (circles, ~49 nm), the buffer is exchanged and the polyprotein is exposed to a solution containing 100 mM methylamine (+MA). At 21 pN, four steps appear which account for the release of the polypeptide sequence trapped by the thioester bonds (arrows). Then, the force is increased again to 115 pN, revealing the complete extension of the molecule. Immediately after, MA is washed out from the fluid chamber and the polyprotein is allowed to fold and reform the thioester bonds for 100 s at 4.5 pN. A 115 pN pulse reveals three ~95 nm steps (empty circles) which correspond with the full extension of Cpa, and one Cpa domain with its thioester bond reformed (circles, ~49 nm). Two more quenches at 3 pN are applied to completely recover the thioester-reformed state in all the four domains, as it can be seen in the 115 pN pulse applied approximately after 800 s of experiment (circles). Then, MA is added again and the force quenched to 24 pN to trigger again the cleavage of the thioester bonds of the polyprotein (arrows).

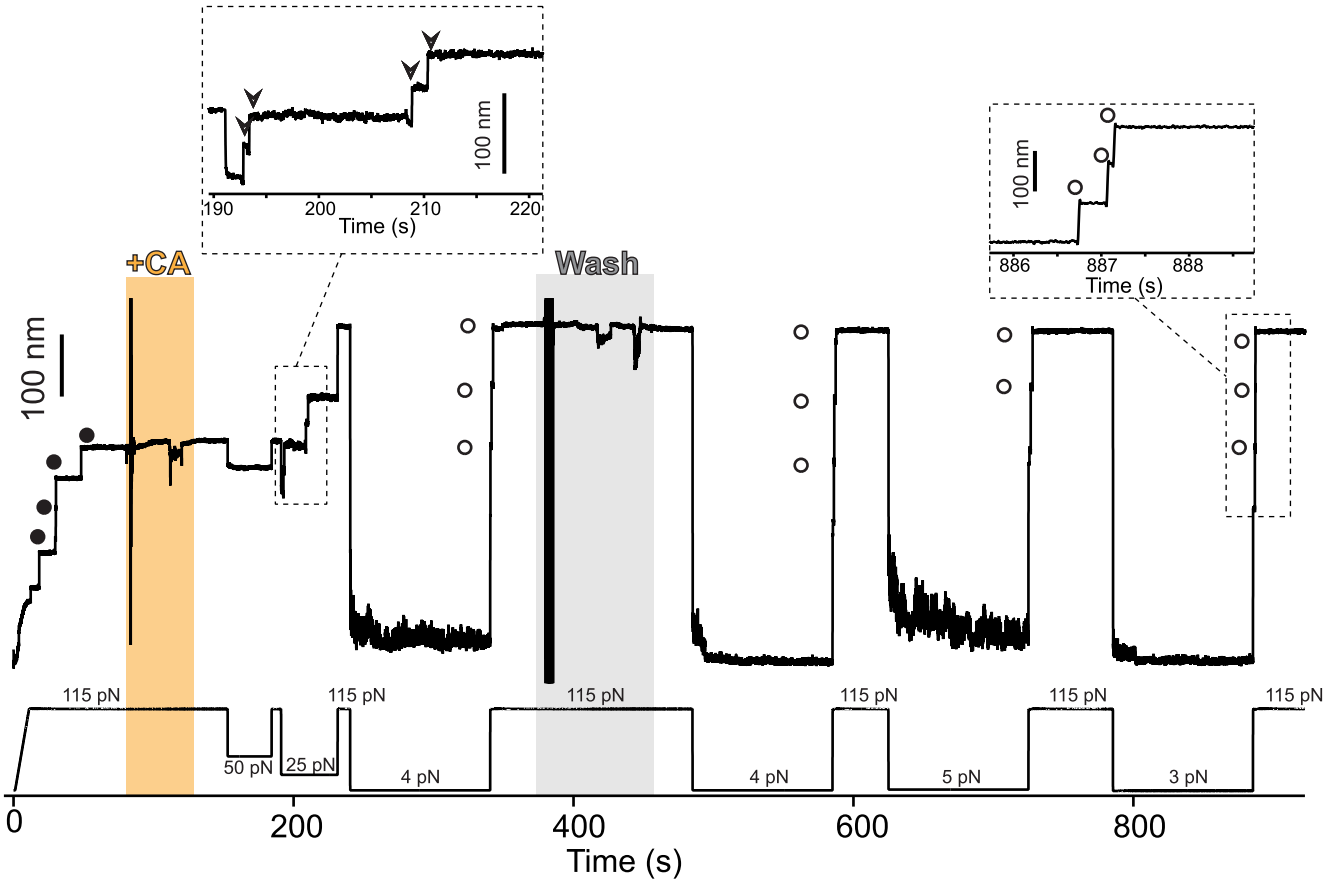


**Extended Data Fig. 2 | Cystamine permanent blocking of Cpa thioester bond reformation.** Magnetic tweezers force-clamp trajectory of the Cpa polyprotein. After the unfolding of the thioester-intact Cpa domains at 115 pN (circles), the buffer is exchanged and the polyprotein is exposed to a solution containing 100 mM cystamine (+CA). At 115 pN and at 50 pN, no additional extensions are registered as a consequence of thioester bond cleavage, but a drop in force to 25 pN leads to the appearance of four steps which account for the release of the polypeptide sequence trapped by the thioester bonds (empty arrows in the inset). Then, the force is increased again to 115 pN, revealing the complete extension of the molecule. After 100 s at 4 pN and in the presence of CA, a 115 pN pulse reveals three ~95 nm steps (empty circles) which correspond with the full extension of Cpa. CA is then removed from the solution, and several consecutive 100 s force quenches (at 4, 5, and 3 pN) followed by 115 pN pulses are applied. These cycles reveal that, after CA treatment, Cpa is able to fold but not to reform its thioester bond, as it can be observed from the ~95 nm steps observed (empty circles). After the first 300 s of the experiment, one of the Cpa domains stops folding back as a consequence of oxidative damage[66]. The disturbances observed in the extension during +CA addition (orange block) and washing (gray block) are originated from the movement of buffer volumes in the liquid cell used in the experiments, which transiently alter the measurement.

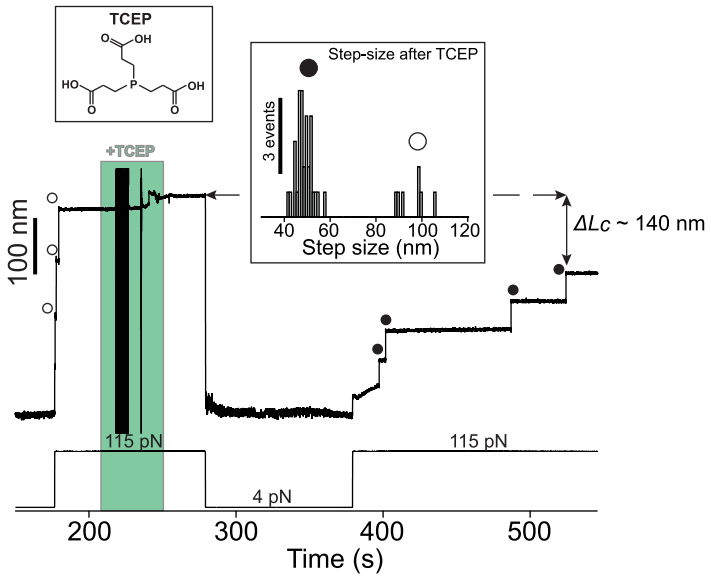


**Extended Data Fig. 3 | TCEP rescues Cpa thioester bond reformation.** A Cpa polyprotein previously treated with cystamine shows three ~95 nm steps at 115 pN corresponding with the full extension of each of the domains (empty circles). The addition of 10 mM TCEP and 100 s at 4 pN is enough to trigger thioester bond reformation, as it can be observed in the ~49 nm thioester-intact Cpa steps (circles) registered at 115 pN. The fourth domain not observed at the beginning was probably unfolded and its thioester bond intact, since the difference in the final extension between the first 115 pN pulse and the last is ~140 nm, which matches with the expected final extension decrease from three reformation events. Inset histogram shows the two populations of steps observed after TCEP treatment, thioester-intact Cpa (circles, 48.3 ± 3.5 nm, mean±SD, n=32) and thioester-cleaved Cpa (empty circles, 95.7 ± 6.4 nm mean±SD, n=7). The latter full length steps of Cpa after TCEP treatment could be due to cleavage events induced by remaining cystamine which was not completely washed from the experimental liquid cell. The disturbances observed in the extension during +TCEP addition (green block) are originated from the movement of buffer volumes in the liquid cell used in the experiments, which transiently alter the measurement.